

Studies on heat capacities and thermal analysis of Li–Mg–N–H hydrogen storage system

F. Xu · L. X. Sun · P. Chen · Y. N. Qi · J. Zhang ·
J. N. Zhao · Y. F. Liu · L. Zhang · Zhong Cao ·
D. W. Yang · J. L. Zeng · Y. Du

Received: 4 April 2009 / Accepted: 11 November 2009 / Published online: 10 December 2009
© Akadémiai Kiadó, Budapest, Hungary 2009

Abstract The heat capacities of LiNH_2 and $\text{Li}_2\text{MgN}_2\text{H}_2$ were measured by a modulated differential scanning calorimetry (MDSC) over the temperature range from 223 to 473 K for the first time. The value of heat capacity of LiNH_2 is bigger than that of $\text{Li}_2\text{MgN}_2\text{H}_2$ from 223 to 473 K. The thermodynamic parameters such as enthalpy ($H-H_{298.15}$) and entropy ($S-S_{298.15}$) versus 298.15 K were calculated based on the above heat capacities. The thermal stabilities of them were investigated by thermogravimetric analysis (TG) at a heating rate of 10 K min^{-1} with Ar gas flow rate of 30 mL min^{-1} from room temperature to 1,080 K. TG curves showed that the thermal decomposition of them occurred in two stages. The order of thermal stability of them is: $\text{Li}_2\text{MgN}_2\text{H}_2 > \text{LiNH}_2$. The results indicate that addition of Mg increases the thermal stability

of Li–N–H system and decrease the value of heat capacities of Li–N–H system.

Keywords Li–Mg–N–H system · MDSC · Heat capacity · TG

Introduction

Light metal-N based materials have been investigated as candidate for hydrogen storage materials. It is generally agreed that lithium nitride (Li_3N) absorbs a total gravimetric density of 10.4 wt% H_2 and volumetric density of about $140 \text{ kg H}_2 \text{ m}^{-3}$ via a two-step reaction and converts to lithium amide (LiNH_2) and lithium hydride (LiH) [1].



Since the hydrogen pressure for the reaction corresponding to the first step is very low, about 0.01 bar at 255 °C [1], only the second step, reaction of Li_2NH with H_2 , will be considered in the current research. The theoretical hydrogen capacity for the second step is 6.5 wt%. Chen et al. [1] pointed out when LiNH_2 and LiH are mixed, H_2 starts to be released at 200 °C reversibly, but the plateau pressure for imide hydrogenation is 1 bar at the relatively high temperature of 285 °C. How to decrease the temperature of hydrogen absorption–desorption for the second step, is important for Li–N based hydrogen storage materials. Nakamori [2] proposed a way for lowering the hydrogen desorption temperatures of Li–N based complex hydride by partial cation substitutions using smaller sized and/or higher valenced cations with larger electronegativities. Therefore, $\text{CaNH}-\text{CaH}_2$, $\text{Mg}(\text{NH}_2)_2-\text{LiH}$ and $\text{LiNH}_2-\text{CaH}_2$ were studied [3–6]. The results indicate that the temperature

F. Xu
Chemistry and Chemical Engineering College, Liaoning Normal University, 850 Huanghe Road, Dalian 116029, People's Republic of China

L. X. Sun (✉) · P. Chen · Y. N. Qi · J. Zhang · J. N. Zhao
Materials and Thermochemistry Laboratory, Dalian Institute of Chemical Physics, Chinese Academy of Sciences, 457 Zhongshan Road, Dalian 116023, People's Republic of China
e-mail: lxsun@dicp.ac.cn

Y. F. Liu
Department of Materials Science and Engineering, Zhejiang University, Hangzhou 310027, People's Republic of China

L. Zhang · Z. Cao · D. W. Yang · J. L. Zeng
School of Chemistry and Environmental Engineering, Changsha University of Science and Technology, Changsha 410076, People's Republic of China

Y. Du
State Key Laboratory of Powder Metallurgy, Central South University, Changsha 410083, People's Republic of China

for hydrogen desorption from these systems are greatly reduced compared with the pure amides and hydrides.

$\text{Li}_2\text{MgN}_2\text{H}_2$ is a promising hydrogen desorption material. The structural and energetic properties of $\text{Li}_2\text{MgN}_2\text{H}_2$ were investigated by the first principle calculation [7]. Isobe [8] studied the hydrogen desorption processes in Li–Mg–N–H system.

The thermodynamic properties such as heat capacity, enthalpy, and entropy are important basic data in chemistry and engineering. Thermodynamic and kinetic properties of Li–Mg–N–H system were investigated. The overall heat and the activation energy of releasing hydrogen from the mixture of $\text{Mg}(\text{NH}_2)_2$ and 2LiH are $44.1 \text{ kJ mol}^{-1} \text{ H}_2$ and 102 kJ mol^{-1} , respectively [9]. To the best of our knowledge, no report about heat capacity, enthalpy, and entropy of the metal-N based materials has been found in the literature. Therefore, it is of great importance to study the thermodynamic properties of the materials for their theoretical and practical purposes.

Modulated differential scanning calorimeter (MDSC) was initially developed by Reading and co-workers in 1992. MDSC is an extension of conventional DSC, in which a sinusoidal wave modulation is applied to the standard linear temperature program. One of the advantages of the MDSC method is its ability to directly determine heat capacities of various materials [10–15]. The structure and principle of the calorimeter have been described in detail in the references [16–18].

LiNH_2 and $\text{Li}_2\text{MgN}_2\text{H}_2$ are reactant and product of LiNH_2 – MgH_2 system, respectively. In this work, thermochemistry characteristics of LiNH_2 and $\text{Li}_2\text{MgN}_2\text{H}_2$ were investigated by using thermogravimetric analysis (TG-DTG) and modulated differential scanning calorimeter (MDSC).

Experimental

Sample

Pure metallic Mg powder, LiH and LiNH_2 were purchased from Sigma-Aldrich. $\text{Mg}(\text{NH}_2)_2$ was synthesized by heating pre-milled Mg powder under purified ammonia atmosphere at a temperature of about $300 \text{ }^\circ\text{C}$ overnight. $\text{Li}_2\text{MgN}_2\text{H}_2$ was synthesized by mixing $\text{Mg}(\text{NH}_2)_2$ with LiH (with molar ratio of 1:2) under Ar atmosphere in a planetary ball mill for 2 days. The XRD curves of the three samples are shown in Fig. 1. By comparing the shapes of these curves with those in references, the results indicated these samples are LiNH_2 [refers to JCPDS (Joint Committee on Powder Diffraction Standards), Index card 75-0049], $\text{Mg}(\text{NH}_2)_2$ and $\text{Li}_2\text{MgN}_2\text{H}_2$

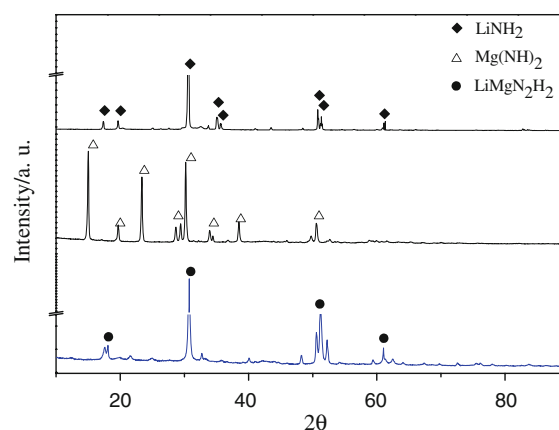


Fig. 1 X-ray diffraction of LiNH_2 , $\text{Mg}(\text{NH}_2)_2$, and $\text{Li}_2\text{MgN}_2\text{H}_2$

(refer to [9]), respectively. Before experiments, LiNH_2 and $\text{Li}_2\text{MgN}_2\text{H}_2$ were held in an argon-filled glove box (M. Braun Co., Germany). These samples were measured by MDSC and TG after they were weighed and sealed in the glove box.

Thermal properties and heat capacity measurement

The thermogravimetry (TG) of the above two kinds of materials were performed using a thermogravimetric analyzer DT-20B instrument (Shimadzu Co., Japan). TG curves were obtained under Ar atmosphere at a heating rate of 10 K min^{-1} from room temperature to $1,080 \text{ K}$. The Ar gas flow rate was 30 mL min^{-1} .

The heat capacities of these materials were measured by MDSC on a Q1000 from TA Instruments, in a temperature range from 223 to 463 K with a heating rate of 3 K min^{-1} . A liquid nitrogen cooling system was used for the experiment temperature control. And dry nitrogen gas was used as a purge gas (50 mL min^{-1}) through the DSC cell.

The temperature of the equipment was initially calibrated in the standard DSC mode, using the extrapolated onset temperatures of the melting of indium (429.75 K) at a heating rate of 10 K min^{-1} . The heat-flow rate was approximately calibrated with the heat of fusion of indium (28.45 J g^{-1}). The heat capacity calibration was made by running a standard sapphire (Al_2O_3) in the experimental temperature range. The calibration method and the experiment were performed at the same conditions as follows: (1) sampling interval: 100 s/pt , (2) zero heat flow at 288.15 K , (3) equilibrate at 173.15 K , (4) modulate temperature amplitude of $\pm 0.5 \text{ K}$ with period of 100 s , (5) isothermal for 5.00 min , and (6) temperature ramp at 3 K min^{-1} to 473.15 K .

Heat capacity constants at $T = 223.15$ to 463.15 K

$$K_{(\text{Total})} = 1.024; \quad K_{(\text{Reversing})} = 1.019.$$

Results and discussion

Heat capacities of standard sapphire ($\alpha\text{-Al}_2\text{O}_3$)

In this article, the heat capacity measurements of each sample are repeated three times unless stated elsewhere. In order to check the accuracy of the used calorimeters (Q1000TM DSC), heat capacities of standard materials like $\alpha\text{-Al}_2\text{O}_3$ have been measured, from 223 to 463 K. The heat capacities are recorded at an interval of $\Delta T = 10$ K for the comparison with the reported values. The experimental precision is below $\pm 0.5\%$. It shows that the testing system of MDSC is steady. The values of experimental heat capacities of $\alpha\text{-Al}_2\text{O}_3$ based on MDSC were compared with the recommended data of the National Institute of Standards and Technology (NIST) [19]. The accuracy for the experimental and the recommended data of the heat capacities of $\alpha\text{-Al}_2\text{O}_3$ is within $\pm 1.5\%$ over the whole temperature range.

Heat capacities of LiNH_2 and $\text{Li}_2\text{MgN}_2\text{H}_2$

The heat capacity is one of the main thermophysical quantities for any material, and its accurate values are needed in many areas of physics, chemistry, and engineering sciences.

Figure 2 shows the heat capacities of LiNH_2 and $\text{Li}_2\text{MgN}_2\text{H}_2$. From Fig. 2, it can be seen that the heat capacities of the two samples increase with the increasing temperature and no phase transition or thermal anomaly was observed in the temperature region from 223 to 473 K. It indicates that the two samples are stable in the above temperature range. The value of heat capacity of LiNH_2 is bigger than that of $\text{Li}_2\text{MgN}_2\text{H}_2$ in 223–473 K.

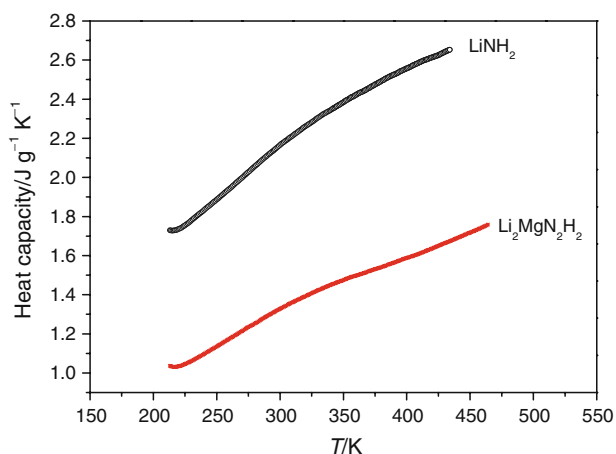


Fig. 2 The curves of C_p vs. T for LiNH_2 and $\text{Li}_2\text{MgN}_2\text{H}_2$

The heat capacities of the above samples are fitted to the Shomate Equation of heat capacities ($C_{p,m}$) with reduced temperature (t) by means of the nonlinear least squares fitting using the OriginPro 7.5 software, at the temperature range from 223 to 473 K for LiNH_2 and $\text{Li}_2\text{MgN}_2\text{H}_2$.

For LiNH_2

$$C_{p,m}(\text{J mol}^{-1} \text{K}^{-1}) = -10.18792 + 72.64769t - 151.315t^2 + 113.6072t^3 + 0.09964/t^2, \quad (3)$$

where $t = T/1,000$ and T (K) is the experimental temperature. The correlation coefficient of the fitting, $R^2 = 0.99998$, $\chi^2/\text{DoF} = 6.43\text{E}-06$ (DoF is the abbreviation of the degree of freedom). Relative deviations of all the experimental points from the fitting heat capacity values for the LiNH_2 are within $\pm 0.8\%$.

For $\text{Li}_2\text{MgN}_2\text{H}_2$

$$C_{p,m}(\text{J mol}^{-1} \text{K}^{-1}) = -9.33276 + 65.3146t - 143.866t^2 + 113.8376t^3 + 0.08455/t^2, \quad (4)$$

where the correlation coefficient of the fitting, $R^2 = 0.99992$, and $\chi^2/\text{DoF} = 3.72\text{E}-06$. Relative deviations of all the experimental points from the fitting heat capacity values for the LiNH_2 are within $\pm 0.6\%$.

Based on the Eqs. 3, 4, the heat capacities of the above samples at 298.15 K were calculated to be 2.153 (LiNH_2) and 1.320 ($\text{Li}_2\text{MgN}_2\text{H}_2$) $\text{J mol}^{-1} \text{K}^{-1}$, respectively.

Thermodynamic functions of LiNH_2 and $\text{Li}_2\text{MgN}_2\text{H}_2$

Enthalpy and entropy of substances are basic thermodynamic functions. The thermodynamic functions relative to the reference temperature of 298.15 K were calculated in the temperature ranges from 223 to 473 K with an interval of 5 K. The thermodynamic relationships are as follows:

$$H_T - H_{298.15} = \int_{298.15}^T C_{p,m} dT = 1,000 \int_{298.15}^t C_{p,m} dt \quad (5)$$

$$S_T - S_{298.15} = \int_{298.15}^T \frac{C_{p,m}}{T} dT = \int_{298.15}^t \frac{C_{p,m}}{t} dt, \quad (6)$$

where $t = T/1,000$. The values of thermodynamic function such as calculated heat capacities, $H_T - H_{298.15}$ and $S_T - S_{298.15}$ are given in Tables 1, 2.

Thermal analysis of LiNH_2 and $\text{Li}_2\text{MgN}_2\text{H}_2$

The TG curves of LiNH_2 and $\text{Li}_2\text{MgN}_2\text{H}_2$ are shown in Fig. 3. These curves indicate the difference of thermal

Table 1 The thermodynamic parameters of LiNH₂

<i>T</i> /K	$C_p^*/J\ g^{-1}\ K^{-1}$	$H-H_{298.15}/J\ g^{-1}$	$S-S_{298.15}/J\ g^{-1}\ K^{-1}$	<i>T</i> /K	$C_p^*/J\ g^{-1}\ K^{-1}$	$H-H_{298.15}/J\ g^{-1}$	$S-S_{298.15}/J\ g^{-1}\ K^{-1}$
215	1.721	-160.2	-0.6261	325	2.283	59.60	0.1913
220	1.739	-151.6	-0.5863	330	2.305	71.07	0.2263
225	1.760	-142.8	-0.5470	335	2.327	82.65	0.2612
230	1.782	-134.0	-0.5081	340	2.347	94.33	0.2958
235	1.807	-125.0	-0.4695	345	2.368	106.1	0.3302
240	1.832	-115.9	-0.4312	350	2.387	118.0	0.3644
245	1.859	-106.7	-0.3931	355	2.406	130.0	0.3984
250	1.886	-97.32	-0.3553	360	2.424	142.1	0.4322
255	1.914	-87.82	-0.3177	365	2.442	154.2	0.4657
260	1.942	-78.18	-0.2802	370	2.459	166.5	0.4991
265	1.971	-68.39	-0.2430	375	2.476	178.8	0.5322
270	1.999	-58.47	-0.2059	380	2.492	191.2	0.5651
275	2.027	-48.40	-0.1689	385	2.508	203.7	0.5978
280	2.055	-38.20	-0.1322	390	2.524	216.3	0.6303
285	2.083	-27.85	-0.0955	395	2.539	229.0	0.6625
290	2.110	-17.37	-0.0591	400	2.554	241.7	0.6945
295	2.137	-6.756	-0.0228	405	2.569	254.5	0.7264
298.15	2.153	0.000	0.0000	410	2.584	267.4	0.7580
300	2.163	3.992	0.0133	415	2.599	280.4	0.7894
305	2.188	14.87	0.0493	420	2.614	293.4	0.8206
310	2.213	25.87	0.0851	425	2.629	306.5	0.8516
315	2.237	37.00	0.1207	430	2.644	319.7	0.8825
320	2.260	48.24	0.1561				

C_p^* is calculated through Eq. 3

stability between the two samples. According to the TG curves (Fig. 3), it seems that two steps mass losses occur with increasing temperature in the experimental temperature range for the above two samples. The weight losses in the first step about the two samples are 6.9% (LiNH₂) from 421 to 595 K and 5.4% (Li₂MgN₂H₂) from 691 to 860 K, respectively. The weight losses for the second step are 31.0% (LiNH₂) up to 776 K and 13.4% (Li₂MgN₂H₂) up to 1,081 K, respectively. Chen et al. [20] considered the decomposition of pure LiNH₂ began around 200 °C. The decomposed products were ammonia at first, and then at higher temperatures N₂ and H₂ released. Therefore, the mass loss of LiNH₂ is ascribed to the decomposition of LiNH₂ to release NH₃, N₂, and H₂. As shown in Fig. 3, the starting temperature of decomposition of LiNH₂ is about 421 K, it may correspond to NH₃ releasing, and then to mixture of NH₃, N₂, and H₂ producing. According to literature [8], the ammonia signal is observed at about 400–500 °C in the curves of TDMS of Li₂MgN₂H₂. Figure 3 shows that the initial temperature of decomposition of Li₂MgN₂H₂ is about 691 K. It indicates Li₂MgN₂H₂ starts decompose to produce NH₃ and should be used under 691 K. The results of the TG analysis demonstrate that the thermal stability of Li₂MgN₂H₂ is higher than that of

LiNH₂. Therefore, the higher thermal stability and lower heat capacity of Li₂MgN₂H₂ product are in favor of hydrogen desorption reaction of LiNH₂-MgH₂ system according to the equation: 2LiNH₂ + MgH₂ ↔ Li₂MgN₂H₂ + 2H₂. The results obtained in the present article are in good agreement with the work of Lou et al. [5].

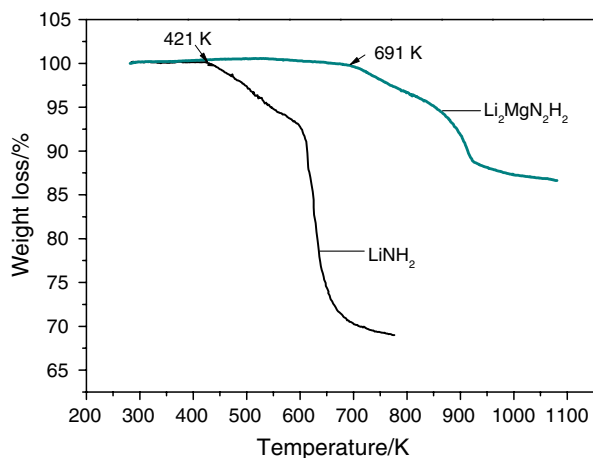
Conclusions

The heat capacity, enthalpy, and entropy of substances are basic thermodynamic functions. Their accurate values are needed in many areas of physics, chemistry, and engineering sciences. The heat capacities of LiNH₂ and Li₂MgN₂H₂ were determined in the temperature range from 223 to 473 K by MDSC. The value of heat capacity of LiNH₂ is bigger than that of Li₂MgN₂H₂ from 223 to 473 K. According to the C_p fitting equation of the two samples, their enthalpy and entropy relative to the reference temperature of 298.15 K were calculated in the temperature ranges from 223 to 473 K, respectively. Their thermal stability was explored by TG from 280 to 1,080 K. The results of TG showed that the order of thermal stability of them is Li₂MgN₂H₂ > LiNH₂. Therefore, the higher

Table 2 The thermodynamic parameters of $\text{Li}_2\text{MgN}_2\text{H}_2$

T/K	$C_p^*/\text{J g}^{-1} \text{K}^{-1}$	$H-H_{298.15}/\text{J g}^{-1}$	$S-S_{298.15}/\text{J g}^{-1} \text{K}^{-1}$	T/K	$C_p^*/\text{J g}^{-1} \text{K}^{-1}$	$H-H_{298.15}/\text{J g}^{-1}$	$S-S_{298.15}/\text{J g}^{-1} \text{K}^{-1}$
215	1.020	-96.78	-0.3778	340	1.449	58.07	0.1821
220	1.032	-91.65	-0.3542	345	1.462	65.35	0.2033
225	1.047	-86.45	-0.3308	350	1.475	72.69	0.2245
230	1.062	-81.18	-0.3077	355	1.487	80.10	0.2455
235	1.080	-75.82	-0.2846	360	1.499	87.56	0.2663
240	1.098	-70.38	-0.2617	365	1.511	95.09	0.2871
245	1.116	-64.85	-0.2389	370	1.522	102.7	0.3077
250	1.136	-59.22	-0.2161	375	1.533	110.3	0.3282
255	1.155	-53.49	-0.1934	380	1.545	118.0	0.3486
260	1.175	-47.66	-0.1708	385	1.556	125.8	0.3689
265	1.195	-41.74	-0.1482	390	1.567	133.6	0.3890
270	1.215	-35.71	-0.1257	395	1.578	141.4	0.4091
275	1.234	-29.59	-0.1033	400	1.589	149.3	0.4290
280	1.254	-23.37	-0.08084	405	1.600	157.3	0.4488
285	1.273	-17.05	-0.05848	410	1.611	165.3	0.4685
290	1.291	-10.64	-0.03619	415	1.623	173.4	0.4881
295	1.309	-4.141	-0.01396	420	1.635	181.6	0.5076
298.15	1.320	0.000	0.000	425	1.647	189.8	0.5270
300	1.327	2.449	0.00819	430	1.660	198.0	0.5463
305	1.344	9.125	0.03026	435	1.673	206.4	0.5656
310	1.360	15.89	0.05224	440	1.687	214.8	0.5848
315	1.376	22.73	0.07414	445	1.702	223.2	0.6039
320	1.392	29.65	0.09594	450	1.717	231.8	0.6230
325	1.407	36.65	0.1176	455	1.733	240.4	0.6421
330	1.421	43.72	0.1392	460	1.750	249.1	0.6611
335	1.435	50.86	0.1607				

C_p^* is calculated through Eq. 4

**Fig. 3** The TG curves of LiNH_2 and $\text{Li}_2\text{MgN}_2\text{H}_2$

thermal stability and lower heat capacity of $\text{Li}_2\text{MgN}_2\text{H}_2$ are in favor of hydrogen desorption reaction of $\text{LiNH}_2\text{-MgH}_2$ system according to the equation: $2\text{LiNH}_2 + \text{MgH}_2 \leftrightarrow \text{Li}_2\text{MgN}_2\text{H}_2 + 2\text{H}_2$.

Acknowledgements The authors gratefully acknowledge the financial support for this work from the National Natural Science Foundation of China (No. 2083309, 20873148, 20903095, 50671098, and U0734005), 863 projects (2007AA05Z115 and 2007AA05Z102), the National Basic Research Program (973 program) of China (2010CB631303) and IUPAC (Project No. 2008-006-3-100).

References

- Chen P, Xiong ZT, Liu J, Tan KL. Interaction of hydrogen with metal nitrides and imides. *Nature*. 2002;420:302–4.
- Nakamori Y, Orimo SI. Destabilization of Li-based complex hydrides. *J Alloys Compd*. 2004;370:271–5.
- Xiong ZT, Chen P, Wu GT, Lin JY, Tan KL. Investigations into the interaction between hydrogen and calcium nitride. *J Mater Chem*. 2003;13:1676–80.
- Xiong ZT, Wu GT, Hu JJ, Chen P. Ternary imides for hydrogen storage. *Adv Mater*. 2004;17:1522–5.
- Lou WF. $(\text{LiNH}_2\text{-MgH}_2)$: a viable hydrogen storage system. *J Alloys Compd*. 2004;381:284–7.
- Leng HY, Ichikawa T, Hino S, Nobuko H, Shigehito I, Hironobu F. New metal-N-H system composed of $\text{Mg}(\text{NH}_2)_2$ and LiH for hydrogen storage. *J Phys Chem B*. 2004;108:12628–30.

7. Araújo CM, Scheicher RH, Jena P, Ahuja R. On the structural and energetic properties of the hydrogen absorber $\text{Li}_2\text{Mg}(\text{NH})_2$. *Appl Phys Lett*. 2007;91:091924.
8. Isobe S, Ichikawa T, Leng H, Fujii H, Kojima Y. Hydrogen desorption processes in Li–Mg–N–H systems. *J Phys Chem Solids*. 2008;69:2234–6.
9. Xiong ZT, Hu JJ, Wu GT, Chen P, Lou WF, Gross K, et al. Thermodynamic and kinetic investigations of the hydrogen storage in the Li–Mg–N–H system. *J Alloys Compd*. 2005;398:235–9.
10. Reading M, Luget A, Wilson R. Modulated differential scanning calorimetry. *Thermochim Acta*. 1994;238:295–307.
11. Swier S, Mele BV. The heat capacity signal from modulated temperature DSC in non-isothermal conditions as a tool to obtain morphological information during reaction-induced phase separation. *Polymer*. 2003;44:6789–806.
12. Divi S, Chellappa R, Chandra D. Heat capacity measurement of organic thermal energy storage materials. *J Chem Thermodyn*. 2006;38:1312–26.
13. Zhang J, Liu YY, Zeng JL, Xu F, Sun LX, You WS, et al. Thermodynamic properties and thermal stability of the synthetic zinc formate dehydrate. *J Therm Anal Calorim*. 2008;91:861–6.
14. Qiu SJ, Chu HL, Zhang J, Qi YN, Sun LX, Xu F. Heat capacities and thermodynamic properties of CoPc and CoTMPP. *J Therm Anal Calorim*. 2008;91:841–8.
15. Zhang J, Zeng JL, Liu YY, Sun LX, Xu F, You WS, et al. Thermal decomposition kinetics of the synthetic complex Pb(1,4-BDC)·(DMF)(H₂O). *J Therm Anal Calorim*. 2008;91:189–93.
16. Wunderlich B, Jin Y, Boller A. Mathematical-description of differential scanning calorimetry based on periodic temperature modulation. *Thermochim Acta*. 1994;238:277–93.
17. Danley RL. New modulated DSC measurement technique. *Thermochim Acta*. 2003;402:91–8.
18. Wunderlich B. The contributions of MDSC to the understanding of the thermodynamics of polymers. *J Therm Anal Calorim*. 2006;85:179–87.
19. Archer DG. Thermodynamic properties of synthetic sapphire (alpha-al₂o₃), standard reference material 720 and the effect of temperature-scale differences on thermodynamic properties. *J Phys Chem Ref Data*. 1993;22:1441–53.
20. Chen P, Xiong ZT, Luo JZ, Lin JY, Tan KL. Interaction between lithium amide and lithium hydride. *J Phys Chem B*. 2003;107:10967–70.